NJC

Accepted Manuscript

This article can be cited before page numbers have been issued, to do this please use: S. Arora, R. Nagpal, P. Chauhan and S. M.S. Chauhan, *New J. Chem.*, 2016, DOI: 10.1039/C6NJ01676F.

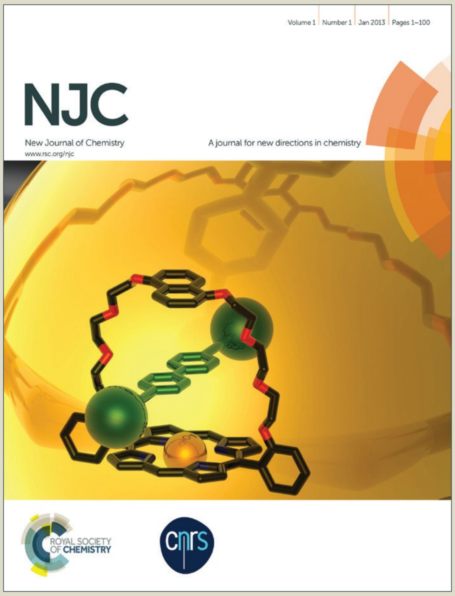

View Article Online
DOI: 10.1039/C6NJ01676F

Journal Name

ARTICLE

Triazole linked Ruthenium(II) porphyrin: Influence of connectivity pattern on photophysical and electrochemical properties

Received 00th January 20xx,
Accepted 00th January 20xx

DOI: 10.1039/x0xx00000x

www.rsc.org/

Smriti Arora, Ritika Nagpal, Prashant Chauhan, Shive Murat Singh Chauhan*

Herein copper catalysed click reaction has been used to covalently link π-conjugated 1,2,3-triazolyl zinc(II) porphyrin and ruthenium(II) bipyridyl with a single change in their connection through the linker. The properties of these compounds have been compared with the porphyrin–ruthenium(II) tris(bipyridine) and ruthenium(II) trisbipyridine complexes. Extensive photophysical and electrochemical studies reveal the changes in electronic properties of the conjugates are a consequence of the different connectivity patterns with regular and inverse triazolyl-pyridyl moieties.

Introduction

In natural photosynthetic systems, porphyrin-based complex serves as the photoactive unit which captures sunlight.[1] To mimic the natural photosynthetic solar energy transduction process, several synthetic porphyrins with large absorption coefficients, multicomponent photoactive arrays in covalent or noncovalent forms have been designed.[2] These mimics incorporate an electron donor, an electron acceptor, and a bridging unit.[3] The donor in many of these systems is a porphyrin or phthalocyanine due to its excellent photophysical and electrochemical properties. The electron acceptor in many model systems is based on Re(I), Ru(II), Os(II), and Cr(III) complexes.[4] Among these, Re(I) and Ru(II), which exhibit high-energy luminescent levels, usually play the role of photosensitizers. The third important unit is linker connecting the two chromophores as mixing a solution of donor and acceptor at micromolar concentrations does not lead to any significant electronic interactions as no efficient quenching of the donor excited state was observed. While introducing a linker between the two units, has a drastic effect on the electron and energy transfer rates of the system.

Supramolecular species (molecular dyads, triads, and tetrads) consisting of metalloporphyrin and ruthenium polypyridine complexes are currently the objective of extensive investigations, as they provide rich photophysical properties which stems from the increase in light harvesting capability as they provide an extentded absorption range favorable for the collection of light.[5] Analogous motifs with improved photophysical and electrochemical properties can be successfully designed by finely-tuning the substituents on porphyrin, nature of the bridge connecting porphyrin and ruthenium chromophores. Previous reports have shown covalent linkage of porphyrin with ruthenium(II) bipyridyl using amide as a linker.[6,7]

Click chemistry is a widely defined tool used for creating several functional ligands for coordination complexes.[8] 1,2,3-triazole moiety, a heterocyclic linking unit is considered to be a premier example capable of coordinating to metal centers in a variety of modes. 1,2,3-triazole has been proved to be a versatile conjugative π-linker to covalently connect two choromophores such as porphyrin-fullerene,[9] porphyrin-graphene,[10] porphyrin-porphyrin.[11] In particular, the copper-catalyzed azide-alkyne cycloaddition (CuAAC) has been used in the synthesis of dendronized linear polymers containing photoactive molecules and in the functionalization of the surface of single-wall carbon nanotubes with polystyrene to solubilize them in a variety of organic solvents.[12] These examples represent interesting applications in molecular electronics, which show the deliberate replacement of bipyridyl with triazolyl-pyridyl[13] should impose interesting electronic properties of the 1,2,3-triazole in the porphyrin-ruthenium(II) macrocycles.[14] In this paper, we have selectively synthesized 1,4-disubstituted 1,2,3-triazoles[15] with a change in mode of connection at 1 and 4 position of triazole giving rise to two different chelators. These chelators were complexed with ruthenium bipyridyl unit to obtain the desired donor-acceptor conjugates. The one coordinating through the more electron rich N3 nitrogen atom of 1,2,3-triazole is a regular triazolyl-pyridyl complex while the one coordinating via N2 nitrogen atom is an inverse triazolyl-pyridyl complex. In order to gain more insight of structure-property relationship, photophysical and electrochemical studies were performed to check the applicability of the novel conjugates.

Results and Discussion

Synthesis and Characterization

Copper(I)-catalyzed azide-alkyne click reaction regioselectively gives 1,4-disubstituted-1,2,3-triazole ring. The clicked ligands **2** (inverse tri-py), **7** (regular tri-py) were synthesized from their corresponding *meso* substituted (*p*-alkynyl or *p*-azido phenyl) porphyrins as shown in Scheme 1. Since, lipid insolubility and aggregation seems to be the major factor in decreasing the efficiency of photosensitizer, 3,5-di-*tert*-butylphenyl groups have been introduced at *meso* positions of the porphyrin ring.[16]

The mono-alkynyl porphyrin was synthesized by mixed-aldehyde condensation using 4-(Trimethylsilyl-

---

Bioorganic Laboratory, Department of Chemistry,
University of Delhi, Delhi-110 007, India.
smschauhan@chemistry.du.ac.in

† Footnotes relating to the title and/or authors should appear here.

Electronic Supplementary Information (ESI) available: [details of any supplementary information available should be included here]. See DOI: 10.1039/x0xx00000x

View Article Online
DOI: 10.1039/C6NJ01676F

ethynyl)benzaldehyde and 3,5-di-*tert*-butylbenzaldehyde with pyrrole in dichloromethane under an argon atmosphere using catalytic amount of boron trifluoride diethyletherate afforded the porphyrinogen, which was oxidized to the corresponding porphyrin using 2,3-dichloro-5,6-dicyano-1,4-benzoquinone (DDQ). The protecting group trimethylsilyl was removed with tetrabutylammonium fluoride (TBAF) to yield alkynylporphyrin (1) and zinc(II) was inserted into the porphyrin using $Zn(OAc)_2$ in chloroform:methanol. The CuAAC between alkynylporphyrin and 2-azidopyridine was performed in the presence of copper sulphate, sodium ascorbate, DIPEA, $CH_2Cl_2/EtOH/H_2O$ **r**efluxed at 50 °C afforded the inverse triazolyl-pyridyl porphyrin **2-Zn** in 85% yield.[17] (Scheme 1)

The synthesis of *p*-azidophenylporphyrin (**6**) also utilized the Lindsey mixed-aldehyde method, with substituting *p*-acetamidobenzaldehyde for ethynylbenzaldehyde.[18] The deacetylation of **4** in presence of EtOH/HCl gave 4-amino-3,5-di-*tert*-butylphenylporphyrin (**5**)[19] which was diazotized by reaction with TFA/$NaNO_2$, followed by *in situ* treatment with NaN_3 to give 4-azido-3,5-di-*tert*-butylphenylporphyrin (**6**).[9a] The porphyrin was clicked[7a] in the presence of copper sulphate, sodium ascorbate, DIPEA, $CH_2Cl_2/EtOH/H_2O$ refluxed at 50 °C afforded with 2-ethynyl pyridine to afford triazolyl-pyridyl porphyrin **7-Zn** in 85% yield. (Scheme 1)

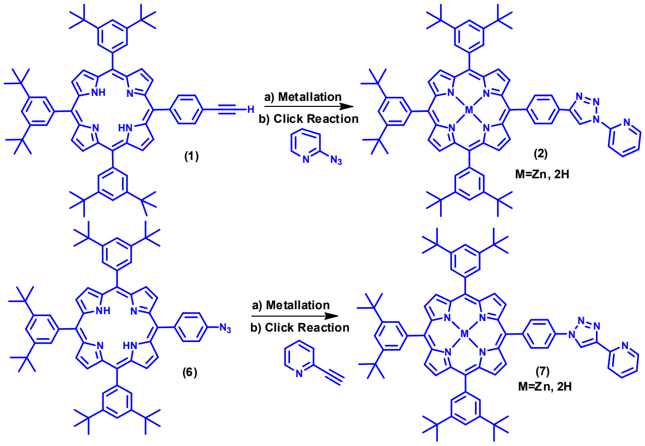

Scheme 1: Synthetic route for chelators: 2-[4-porphyrinyl-1*H*-1,2,3-triazol-1-yl]pyridine (2,2-Zn, inverse tri-py) and 2-[1-porphyrinyl-1*H*-1,2,3-triazol-4-yl]pyridine (7,7-Zn, regular tri-py)

The click reaction of free base alkyne porphyrin (**1**) and azido porphyrin (**6**) gave the corresponding 1,2,3-triazole in low yield. Therefore, the metal free conjugates were synthesized by removal of zinc metal from triazolyl porphyrin **2-Zn** and **7-Zn** under mildly acidic conditions at room temperature in 90% yield.[20]

Heteroleptic triazole chelators on refluxing with a requisite stoichiometry of cis-dichlorobis(2,2'-bispyridyl)ruthenium(II) in EtOH/THF gave the corresponding octahedral complex in ~20% yield.[21] (Scheme 2)

The formation of Ru(II)-octahedral complexes were apparent from the three resonance signals in ^{1}H NMR at δ 1.5 ppm (*tert*-butyl H), 7.96-7.33 ppm (bipyridyl H), a triazole H singlet at 8.42 ppm in **3-Zn** and 8.52 ppm in **8-Zn** (shifted upfileld as compared to the triazolyl porphyrin), β-pyrrolic H's at 8.74 ppm in **3-Zn** and 8.84 ppm in **8-Zn**. Complete ^{1}H NMR are shown in supplementary data (Figure S8,S16) while partial NMR are presented in Figure 1. The assignment of peaks in the ^{1}H NMR spectrum of conjugates was aided by COSY NMR spectrum (Figure 2). Different pattern for β-porphyrinic protons was observed for metallated and base free conjugates which may be attributed to different orientations of the two compounds.

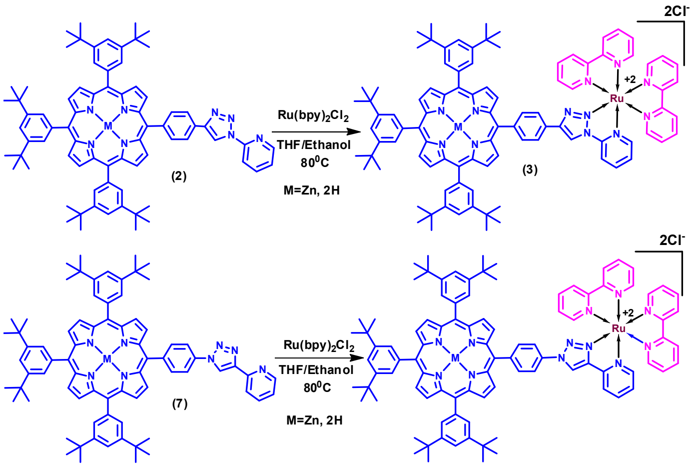

.**Scheme 2**: Synthetic route for Ru(II) bidentate complexes

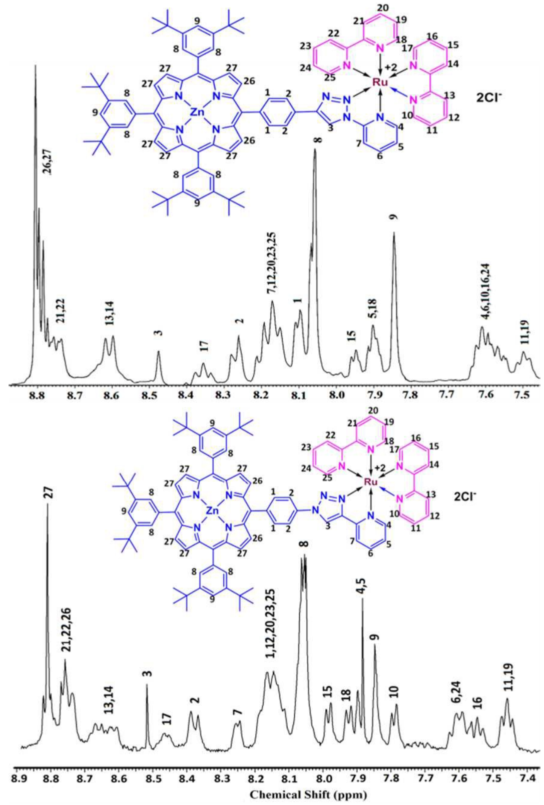

Figure 1: ^{1}H NMR spectrum of 3-Zn, and 8-Zn in Methanol-*d*

1,2,3-triazoles have proved to show interesting hydrogen bonding due to their large polarity (dipole moment ~5D), with the positive end of the dipole situated at the CH group.[22] The triazolyl-

View Article Online
DOI: 10.1039/C6NJ01676F

pyridyl ligand (**7**) shows intramolecular H-bonding (triazolo-4H and Py-N) in non-polar solvent replaced by ligand-solvent H-bonding in polar solvent as depicted by the downfield shift in ^{1}H NMR, bathochromic shift in UV visible spectra on addition of MeOH (Figure S28).

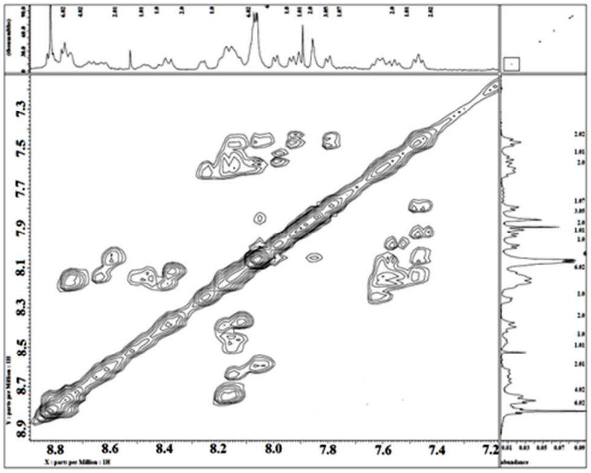

Figure 2: COSY spectrum of 8-Zn in Methanol-*d*

The structure was further confirmed by MALDI-TOF mass spectrometery which shows loss of neutral ligands, charge reduction, and association with a counterion, in addition to the peaks from Zn triazolyl-pyridyl porphyrin (Figure 3). Fragmentation proceeds with loss of Zn which is rarely observed, indicating that demetalation is affected by the linker as well as the substituents on the porphyrin ring.[23]

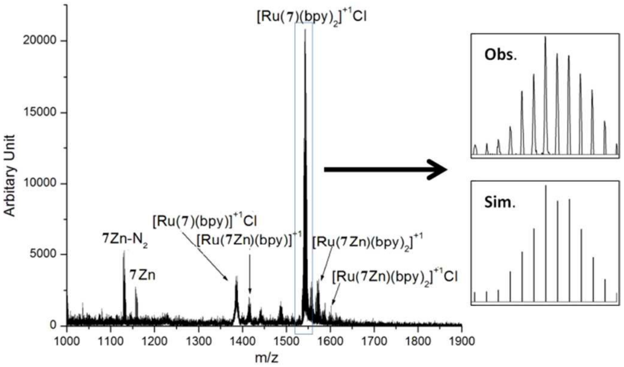

Figure 3: MALDI-TOF mass spectrum of 8-Zn

Photophysical Properties

Figure 4 depicts ground state absorption spectra of the four ruthenium(II)-porphyrin complexes in dichloromethane under ambient conditions. The free base porphyrin-ruthenium(II) conjugates, show intense Soret band ($S_0 \rightarrow S_2$ transition) ~ 424 nm and four Q bands ~ 500-700 nm ($S_0 \rightarrow S_1$ transition), respectively. Introduction of a Zn (II) ion to the porphyrin conjugate, results in small red shift of the Soret band and the number of Q bands were reduced from four to two. In addition to this typical pattern, absorption bands from ruthenium bipyridyl moiety ~ 285-295 nm (bpy π-π^*) were observed which were blue shifted in **3** as compared to **8**. In **8**, **8-Zn**, the metal to ligand charge transfer absorptions around 450 nm associated with the peripheral ruthenium complexes indicate energy transfer from $[Ru(bpy)_2Cl]^+$ triplet states to the lowest energy triplet state of the zinc porphyrin, while in **3**, **3-Zn** relatively low intensity band is observed. This conclusion is supported by the fact that the emission spectrum obtained by excitation at 450 nm, i.e. in the MLCT band of the ruthenium complexes, exhibits essentially the strongly quenched porphyrin emission.[24,25] However, the weaker MLCT band in **3-Zn** shows a weaker electronic communication in ground state between ruthenium bipyridyl and porphyrin moiety.

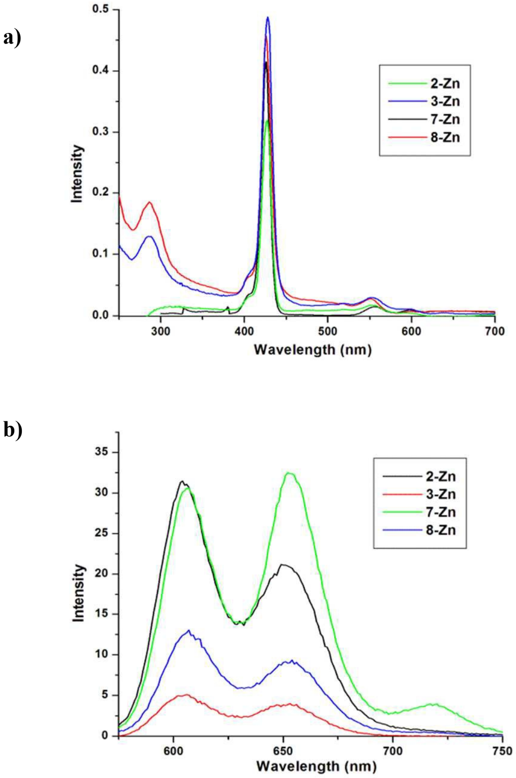

Figure 4: UV visible spectra a) 2-Zn, 3-Zn (2.4*10^{-6}M); 7-Zn,8-Zn (4.0*10^{-6}M) and fluorescence ($\lambda_{max=}$ 420 nm) b) 2-Zn, 3-Zn (2.4*10^{-6}M); 7-Zn,8-Zn (4.0*10^{-6}M) spectra of ruthenium(II)-porphyrin conjugates

The relative emission profile of the metallated dyad **3-Zn** is strongly quenched to about 80 %, 40 % when excited at 420 nm and 550 nm, with respect to the triazole porphyrin **2-Zn** (Table 1). The data show that the electron transfer occurs to a much higher extent in **3-Zn** as compared to other conjugates. These results are in agreement with the fluorescence quantum yields. Similar results are observed with **7-Zn**, **8-Zn** as well. A significantly higher quenching when excited at 420 nm, Soret band, proves that only half of the S_2 population gets back to S_1, while the other half goes via. different pathway. Hence, the emission and absorption profile comparison demonstrates efficient electronic communication in the excited state while no ground-state interaction between porphyrin and ruthenium bipyridyl is observed.

View Article Online
DOI: 10.1039/C6NJ01676F

Table 1: Steady-state emission spectroscopic properties of 2-[1-porphyrinyl-1*H*-1,2,3-triazol-4-yl]pyridine, 2-[4-porphyrinyl-1*H*-1,2,3-triazol-1-yl]pyridine and its ruthenium complexes.

Entry	λ_{abs} (nm) (log ε)	λ_{em}^{a}/nm (Int./a.u.)	λ_{em}^{b}/nm (Int./a.u.)	λ_{em}^{c}/nm (Int./a.u.)	Φ_{em}^{d}	Φ_{em}^{e}
2	422(5.48), 519(4.08), 556(3.78), 594(3.68), 650 (3.62).	653(102.2), 719(26.5)	-	653 (4.46), 719 (1.22)	0.00093	0.048
2-Zn	426(5.38), 553(4.25), 597 (3.50)	604(31.47), 651 (21.22)	-	605 (3.30), 651 (1.89)	0.00055	0.059
3	288(4.63), 424(5.42), 520(4.02), 555(3.80), 594(3.51), 650 (3.48)	652 (57.69), 719(14.06)	654 (0.65), 719 (0.17)	653 (2.78), 719 (0.70)	0.00059	0.036
3-Zn	286 (4.70), 427 (5.31), 554 (4.10), 598 (3.60)	604(5.04), 652(3.96)	606 (0.12), 654 (0.098)	604 (1.67), 655 (1.20)	0.000115	0.039
7	424(5.57), 520(4.05), 557(3.75), 595(3.68), 651(3.66)	652(11.15), 719(3.23)	-	655(0.34), 720(0.11)	0.0027	0.174
7-Zn	426(5.29), 553(3.92), 598(3.60)	596(31.2), 648(36.1)		597(3.09), 647(3.11)	0.00033	0.043
8	295(4.71), 425(5.53), 521(4.05), 556(3.67), 596(3.60), 651(3.66)	653(9.45), 719(2.20)	656(1.26), 719(0.35)	655(0.28), 720(0.11)	0.0023	0.137
8-Zn	290(4.81), 427(5.26), 552(4.0), 598(3.89)	597(12.7), 647(11.6)	600(0.08), 652(0.10)	598(2.84), 647(2.41)	0.00017	0.0406

[a]λ_{ex} = 420 nm, [b]λ_{ex} = 450 nm, [c]λ_{ex} = 550 nm, [d]Emission quantum yields (λ_{em} = 550-800 nm, λ_{ex} = 420 nm), [e]Emission quantum yields (λ_{em} = 560-800 nm, λ_{ex} = 550 nm), Emission quantum yields are measured with ZnTPP as standard.

The inverse (**3**, **3-Zn**) and regular (**8**, **8-Zn**) complexes show different stability towards sunlight. Acetonitrile solutions of both the complexes were monitored by UV visible spectroscopy. The intensity of Soret band due to porphyrin decreases slowly while the absorption band for Rubpy moiety persists for **3**, **3-Zn** when kept in sunlight for more than 24 hours while no changes in UV visible were observed for **8**, **8-Zn** over the same time period. Interestingly, no changes in the absorption spectrum were observed for the same complexes kept in dark. Thus, complexes even being structurally same but ligand exchange studies indicate the regular Ru(II)-tripy complex are more stable than their inverse analogues. These results are consistent with previously performed studies.[26]

.

View Article Online
DOI: 10.1039/C6NJ01676F

Electrochemistry

The redox properties of metal free triazole porphyrin-ruthenium bipyridyl conjugates (**3**, **8**), their zinc counterparts (**3-Zn**, **8-Zn**) were studied by means of cyclic voltammetry in anhydrous dichloromethane using tetra-n-butylammonium hexafluorophosphate (TBAPF$_6$) as the supporting electrolyte and ferrocene/ferrocinium (Fc/Fc$^+$) as the internal reference, platinum wire as counter electrode, glassy carbon electrode as working electrode (~0.25 cm^2), and Ag/Ag$^+$ as reference electrode, respectively. The half-wave potentials, E$_{1/2}$, were determined as (E$_{pa}$ + E$_{pc}$)/2, where E$_{pa}$ and E$_{pc}$ are the anodic and cathodic peak potentials determined from the CV measurements are given in Table 2 alongwith redox potentials of the related compounds.

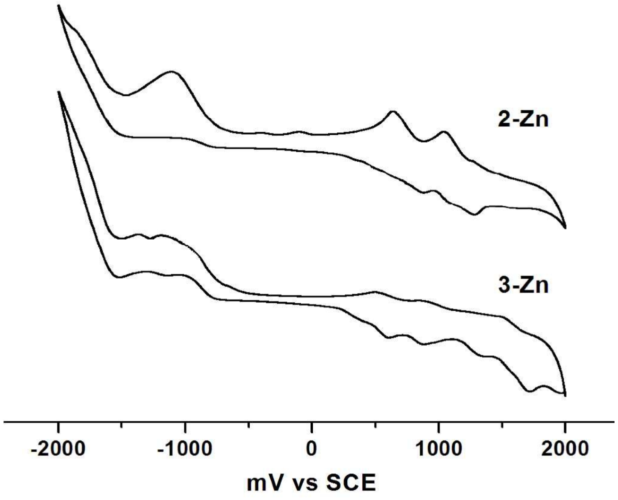

Figure 5: Cyclic voltammogram (CV) of 8-Zn, 3-Zn in CH$_2$Cl$_2$(2*10^{-3} M) with a scan rate of 50 mV/s (0.1 MTBAPF$_6$)

Table 2. Electrochemical data versus SCE for complexes and model compounds

Entry	Ist Oxid.	IInd Oxid.	IIIrd Oxid.	IVth Oxid.	Ist Red.	IInd Red.	IIIrd Red.	[a]Band Gap (E$_g$)
inv-pytri	1.40	[b]	[b]	[b]	-1.24	-1.43	-1.79	2.64
2-Zn	0.75	1.15	[b]	[b]	-0.93	-1.66	[b]	1.68
3	0.63	0.74	1.08	1.35	-1.10	-1.55	[b]	1.73
3-Zn	0.54	0.87	1.32	[b]1.60	-0.97	-1.26	[b]	1.51
reg-pytri	1.32	[b]	[b]	[b]	-1.28	-1.49	-1.96	2.60
7-Zn	0.81	1.12	[b]	[b]	-0.77	-1.29	[b]	1.58
8	0.68	1.16	[b]	[b]	-0.99	-1.55	[b]	1.67
8-Zn	0.40	0.74	1.16	[c]1.46	-0.86	-1.54	[b]	1.26
Ru(bpy)$_3$	1.30	[b]	[b]	[b]	-1.32	-1.51	-1.76	2.67
Ru-amide[23] Zn-Porphyrin	0.78	1.17	1.68	[b]	-0.79	-1.07	-1.43	1.57

[a] Calculated by difference of HOMO and LUMO, all the spectra are measured in CH$_2$Cl$_2$; HOMO-LUMO: ΔE = E^{1st} oxidation -E^{1st} reduction; [b] Peaks donot appear; [c] irreversible peak

In the investigated chemical window (-2.0 to 2.0 V) a reversible cyclic voltagram is observed for all the four compounds. The electrochemical response of 3-Zn (Figure 5), 8-Zn (Figure S26) show four reversible oxidation peaks ranging from 0.40 V to 1.60 V vs SCE which were anodically shifted between 0.63 V to 1.50 V in the case of metal free counterparts 3, 8 (Figure S27). The first two oxidation peaks correspond to the oxidation of ZnP while the fourth peak is assigned to metal-based oxidation (Ru^{2+}/Ru^{3+}) couple making the complex to facilitate electron/energy transfer by generation of porphyrin π-cation radical upon photoexcitation of the Ru subunit. Whereas reduction peaks at E$_{1/2}$ = -0.86 V, -1.54 V in **8-Zn** were observed showing that stepwise electrode processes occur between the bipyridyl ligands and ZnP units of the **8-Zn** complex. Similarly for zinc free counterpart, **8** reversible reduction peaks at -0.99 V, -1.55 V were observed.

Electrochemistry in dichoromethane changes with ligand variation in regular ruthenium(II) complexes (Table 2). Synthesized porphyrin-ruthenium(II) complexes are comparatively easy to reduce as compared to archetypal Ru(bpy)$_3$. Considering the structure of porphyrin complexes synthesized, the inverse triazolyl-pyridyl complexes **3**, **3-Zn** shows a cathodic shift of 220 mV, 210 mV for E°$_{red1}$. The effect of a regular triazole ligand **8**, **8-Zn** is a large cathodic shift of 330 mV, 460 mV for E°$_{red1}$. This shift indicates that the conjugates **3**, **3-Zn** are slightly harder to reduce than the compounds in which porphyrin is connected to the nitrogen of the triazole ring. Hence, the reducability sequence for the porphyrins is 3-Zn>3>8>8-Zn>Ru(bpy)$_3$ for the first reduction process. These results are consistent with the poorer electron donating ability than their regular analogues.[26]

View Article Online
DOI: 10.1039/C6NJ01676F

Replacement of a bipyridyl unit with triazolyl-pyridyl results in a smaller HOMO/LUMO energy gap as observed in **3-Zn**, **8-Zn** compared to a previously reported Zn-Ruamide[27] species. HOMO/LUMO band gap variation also goes along with the differences in the ground state conjugation depending on the connectivity pattern at triazole. When ZnP is attached directly to the triazole N, ground state conjugation is interrupted as the charge transfer resonance structure has cationic character due to the formation of a quaternary ammonium centre. A narrower HOMO/LUMO gap in **8**, **8-Zn** as compared to **3**, **3-Zn**, is observed which would increase the electronic coupling, thus, increasing the charge transfer in conjugates. In general a linear increase in HOMO-LUMO gap with the donor-acceptor distance has been observed.[9b]

A smaller band gap is observed for the zinc-metallated conjugates compared to their unmetallated counterparts, **8-Zn** (E_g = 1.26 eV) compared to **8** (E_g = 1.67 eV), in agreement with the red shift of the absorption spectrum.[17] All these observations show that type of linker and metal has an important influence on the LUMO energy level.[28]

Conclusions

Clicked triazole porphyrin ligands **7, 7-Zn** and their corresponding heteroleptic Ru(II) conjugates **8, 8-Zn** with electron donor and acceptor fragments were synthesized. Triazolyl group acts as a bridging framework for interesting photo-induced electron or energy transfer process between porphyrin and Ru bpy. The properties of these inverse and regular complexes have been compared with Ru(bpy)$_3$ and previously reported porphyrin ruthenium complexes. Photophysical and electrochemical studies clearly demonstrates that the energies of the orbital in the conjugates depend on (1) ligand/linker, (2) connecting pattern of linker, (3) the presence of Zn metal ion in the porphyrin core. Though structurally same but ligand exchange studies indicate the regular Ru(II)-tripy complex are more stable than their inverse analogues. The change in linker provides new insights for the design of more efficient sensitizers for dye sensitized solar cells and optoelectronic devices.

Experimental

The IR spectra were recorded on a Perkin Elmer 1710 FTIR spectrometer and the ν_{max} was expressed in cm^{-1}. The absorption spectra were recorded on a Perkin Elmer Lambda-35 UV/Vis spectrophotometer and the λ_{max} was expressed in nanometers. The ^{1}H NMR spectra were recorded on Bruker Avance-400 spectrometer using TMS as internal standard (chemical shifts in ppm). Fluorescence spectra were recorded on Varian Cary fluorescence spectrometer. MALDI Spectra were recorded on MS - ABI Sciex 5800 TOF/ TOF System with LC-MALDI in cinnamic acid matrix. ESI-MS spectra were recorded on Agilent Technologies 6530 Accurate-Mass Q-TOF LC/MS. Cyclic voltammograms of the samples were obtained using CHI 600D electrochemical analyzer. The compounds were purified using silica gel (60-120 mesh), neutral alumina chromatography.

Synthesis

2-[5-(4-phenyl)-10,15,20-tris(3,5-di-tert-butylphenyl)porphyrinato zinc]-1H--1,2,3-triazol-1-yl pyridine **(2-Zn)**

Porphyrin 1 was metallated by dissolving zinc acetate (0.18 g, 0.83 mmoles) in 1:1 MeOH/CHCl$_3$ (50 mL), reaction was refluxed for 1 h and the crude mixture was washed three times with water. The organic layer was dried over Na$_2$SO$_4$ and filtered. Zn alkyne porphyrin (311 mg, 0.319 mmoles) was added to a mixture of pyridyl azide (35 mg, 0.291 mmoles), CuSO$_4$.5H$_2$O (11.25 mg, 543.83 mmoles), sodium ascorbate (18.03 mg, 432.19 mmoles), DIPEA (117.91 µL, 282.62 mmoles) in DCM/H$_2$O/EtOH (5:2:1) (60 mL) and stirred at 50 °C for 12 h. After cooling, the reaction mixture was diluted with CH$_2$Cl$_2$ (20 mL) and washed with water. The resulting organic layer was dried over Na$_2$SO$_4$ and evaporated to dryness. The residue was purified by silica gel coloumn chromatography using 7:3 CHCl$_3$/petroleum ether as eluent to yield the desired product in 85% yield (0.314 g).

R$_f$: 0.5 (CHCl$_3$); UV−visible (CHCl$_3$), λ_{abs}/nm (log ε): 426 (5.38), 553 (4.25), 597 (3.50); ^{1}H NMR (400 MHz, Chloroform-*d*) δ ppm 9.1-8.95 (m, 8H, βH), 8.59 (s, triazole H, 1H), 8.38-8.30 (m, 5H, ArH, PyH), 8.10 (m, 6H, ArH), 8.00 (t, 1H, PyH), 7.78 (s, 3H, ArH), 7.42 (t, 1H, PyH), 1.51 (s, 54H, *t*-butyl); ^{13}C NMR (100 MHz, Chloroform-*d*) δ ppm: 150.5, 150.5, 150.3, 148.6, 143.4, 141.9 139.4, 135.0, 132.5, 132.3, 132.2, 131.7, 129.8, 129.7, 124.2, 122.5, 120.8, 117.2, 115.9, 114.0, 35.1, 31.7; MALDI calculated 1156.5797 ($C_{75}H_{82}N_8Zn$), observed 1095.6741 (M-Zn+H)$^+$, 1067.9371 (M-Zn-N$_2$).

2-[5-(4-phenyl)-10,15,20-tris(3,5-di-tert-butylphenyl)porphyrinato zinc]-1H-1,2,3-triazol-1-yl-pyridine 2,2'-bispyridine ruthenium(II) chloride **(3-Zn)**

Porphyrin (2-Zn) (0.030 g, 0.0258 mmoles) and cis-Ru(bpy)$_2$Cl$_2$ (6) (37 mg, 0.077 mmol) were added in a mixture of THF (8 mL) and EtOH (8 mL). The solution was bubbled with N$_2$ for a few minutes, and heated to 85 °C. After refluxing for 15 h, the solvent was removed under vacuum to dryness. The residue was chromatographed on neutral Al$_2$O$_3$. Brown coloured band was collected using CHCl$_3$:MeOH (v/v) = 10:1 as eluent to give 3-Zn in 20 % yield (8.54 mg).

R$_f$: 0.3 (10% MeOH : CHCl$_3$); UV Vis. (CHCl$_3$), λ_{abs}/nm (log ε): 286 (4.70), 427 (5.31), 554 (4.10), 598 (3.60); ^{1}H NMR (400 MHz, Metahnol-*d*) δ ppm : 8.76-8.65 (m, 10H, βH, PyH), 8.69-8.55 (m, 2H, Py H), 8.42 (s, 1H, triazole H), 8.18-8.15 (m, 2H, ArH), 8.10-8.00 (m, 4H, ArH, PyH), 8.0-7.9 (m, 8H, ArH, PyH), 7.83-7.7 (m, 8H, ArH, Py H), 7.65-7.62 (d, 1H, PyH), 7.58-7.41 (m, 5H, PyH), 7.38-7.31 (m, 1H, PyH), 1.51 (s, 54 H, *t*-butyl); MALDI: calculated 1640.5593 ($C_{95}H_{96}Cl_2N_{12}RuZn$), observed 1543.6771 [(Ru(2)(bpy)$_2$]$^+$Cl.

2-[5-(4-phenyl)-10,15,20-tris(3,5-di-tert-butylphenyl)porphyrinyl]-1H-1,2,3-triazol-1-yl pyridine **(2)**

View Article Online
DOI: 10.1039/C6NJ01676F

Porphyrin (2-Zn) (0.050 g, 0.043 mmoles) in CH_2Cl_2 (15 mL) was added HCl in dioxane (20 M, 2.5 mL), stirred at r.t. for 5 min. The mixture was neutralised with saturated $NaHCO_3$ solution, dried over sodium sulphate, and the solvent was removed under reduced pressure to yield the product in 90% yield (0.045g).

R_f : 0.5 ($CHCl_3$); UV−visible ($CHCl_3$), λ_{abs}/nm (log ε) 422 (5.48), 519 (4.08), 556 (3.78), 594 (3.68), 650 (3.62); ^1H NMR (400 MHz, Chloroform-*d*) δ ppm 9.1-8.85 (m, 8H, βH), 8.60 (s, 1H, triazole H), 8.40-8.32 (m, 5H, ArH, PyH), 8.15-8.06 (m, 6H, ArH), 8.00 (t, 1H, PyH), 7.80 (s, 3H, ArH), 7.42 (t, 1H, PyH), 1.51 (s, 54H, *t*-butyl), -2.40 (s, 2H, -NH); ^{13}C NMR (100 MHz, Chloroform-*d*) δ ppm: 148.8, 148.7, 148.6, 141.3, 139.4, 137.3, 135.2, 131.9, 129.9, 129.7, 129.8, 125.5, 124.3, 123.8, 121.5, 121.1, 117.3, 116.7, 116.1, 114.0, 35.1, 31.8; MALDI calculated 1094.6662 ($C_{75}H_{82}N_8$), observed 1095.6741 $(M+H)^+$, 1067.9451 ($M-N_2$).

2-[5-(4-phenyl)-10,15,20-tris(3,5-di-tert-butylphenyl)porphyrinyl]-1H-1,2,3-triazol-1-yl-pyridine-2,2'-bispyridine ruthenium(II) chloride (3)

Porphyrin (2) (0.040 g, 0.0365 mmoles) and cis-Ru(bpy)$_2$Cl$_2$ (6) (0.0523 g, 0.108 mmol) were added in a mixture of THF (6 mL) and EtOH (6 mL). The solution was then bubbled with N_2 for a few minutes, and heated to 85 °C. After refluxing 15 h, the solvent was removed under vacuum and the residue was chromatographed on neutral Al_2O_3 and the last brown band was collected, using $CHCl_3$:MeOH (v/v) = 10:1 as eluent (18 % yield ~ 10.47 mg).

R_f : 0.3 (10% MeOH : $CHCl_3$); UV Vis. ($CHCl_3$), λ_{abs}/nm (log ε): 288 (4.63), 424 (5.42), 520 (4.02), 555 (3.80), 594 (3.51), 650 (3.48); ^1H NMR (400 M Hz, Metahnol-*d*) δ ppm : 8.85-8.76 (m, 8H, βH), 8.69-8.60 (m, 2H, PyH), 8.52 (s, 1H, triazole H), 8.41-8.35 (m, 1H, PyH), 8.27 (m, 2H, ArH), 8.22-8.18 (m, 4H, ArH,PyH), 8.10 (m, 1H, PyH), 8.05 (s, 6H, ArH), 7.96-7.89 (m, 6H, ArH), 7.65-7.49 (m, 6H, PyH), 7.23-7.19 (t, 2H, *J*= 8 Hz, PyH), 7.11 (d, 2H, *J*= 8 Hz, Py H), 1.51 (s, 54 H, *t*-butyl); MALDI: calculated 1578.6458 ($C_{95}H_{98}Cl_2N_{12}Ru$), observed 1543.6458 $[(Ru(2)(bpy)_2]^+Cl$.

2-[5-(1-phenyl)-10,15,20-tris(3,5-di-tert-butylphenyl)porphyrinato zinc]-1H-1,2,3-triazol-4-yl)pyridine (7-Zn)

Zinc acetate (0.18 g, 0.83 mmoles) was dissolved in 1:1 MeOH/$CHCl_3$ (50 mL) and added to porphyrin 6. The reaction was refluxed for 1 h and the crude mixture was washed three times with water. The organic layer was dried over Na_2SO_4 and filtered. 2-ethynyl pyridine (75.83 µL, 365.31 mmoles) was added to a mixture of Zn porphyrin (0.200 g, 0.195 mmoles), $CuSO_4.5H_2O$ (7.25 mg, 349.85 mmoles), sodium ascorbate (11.6 mg, 278.06 mmoles), DIPEA (75.83 µL, 181.76 mmoles) in DCM/H_2O/EtOH (5:2:1) (60 mL) and stirred at 50 ℃ for 12 h. After cooling, the reaction mixture was diluted with CH_2Cl_2 (20 mL) and washed with water. The resulting organic layer was dried over Na_2SO_4 and evaporated to dryness. The residue was purified by silica gel coloumn chromatography using 7:3 $CHCl_3$/petroleum ether as eluent to yield the desired product in 85% yield (0.198 g).

R_f : 0.3 ($CHCl_3$); UV−visible ($CHCl_3$) λ_{abs}/nm (log ε): 427 (5.65), 556 (4.32), 598 (4.02); ^1H NMR (400 MHz, Chloroform-*d*) δ ppm: 8.93-9.04 (m, 8H, βH), 8.70 (s, 1H, triazole H), 8.45 (m, 1H, Py H), 8.40 (d, *J*= 7.48 Hz, 2H, ArH), 8.25 (d, *J*= 9.56 Hz, 1H, PyH), 8.15 (d, *J*= 7.48 Hz, 2H, ArH), 8.05 (s, 6H, ArH), 7.85 (t, *J*= 8.56 Hz, 1H, PyH), 7.81 (s, 3H, ArH), 7.10 (dd, *J*= 7.48 Hz, 1H, PyH), 1.51 (s, 54H, *t*-butyl); ^{13}C NMR (100 MHz, Chloroform-*d*) δ ppm: 150.5, 150.4, 150.3, 149.6, 149.1, 148.5, 141.8, 139.2, 137.0, 136.1, 135.4, 132.5, 132.3, 132.2, 131.1, 129.7, 129.6, 122.6, 120.7, 120.5, 119.9, 118.4, 35.0, 31.7; MALDI: calculated 1156.5797 ($C_{75}H_{80}N_8Zn$), observed 1094.6662 (7-Zn), 1066.6601 (7-N_2).

2-[5-(1-phenyl)-10,15,20-tris(3,5-di-tert-butylphenyl)porphyrinato zinc]-1H-1,2,3-triazol-4-yl-pyridine 2,2'-bispyridine ruthenium(II) chloride (8-Zn)

Porphyrin (7-Zn) (0.030 g, 0.0258 mmoles) and cis-Ru(bpy)$_2$Cl$_2$ (6) (37 mg, 0.077 mmol) were added in a mixture of THF (8 mL) and EtOH (8 mL). The solution was bubbled with N_2 for a few minutes, and heated to 85 °C. After refluxing for 15 h, the solvent was removed under vacuum to dryness. The residue was chromatographed on neutral Al_2O_3. Brown coloured band was collected using $CHCl_3$:MeOH (v/v) = 10:1 as eluent to give 8-Zn in 19 % yield (8.09 mg).

R_f : 0.2 (10% $CHCl_3$: MeOH); UV Vis. ($CHCl_3$), λ_{abs}/nm (log ε): 286 (4.81), 427 (5.26), 552 (4.0), 598 (3.89); ^1H NMR (400 MHz, Methanol-*d*) δ ppm : 8.70-8.84 (m, 10H, βH, PyH), 8.6-8.7 (m, 2H, PyH), 8.52 (s, 1H triazolyl H), 8.45 (m, 1H, PyH), 8.37 (d, *J*= 6.8 Hz, 2H, ArH), 8.25 (d, *J*=4.6 Hz, 1H, PyH), 8.15 (m, 6H, ArH, PyH), 8.05 (m, 6H, ArH), 7.98 (d, *J*= 5.36 Hz, 1H, PyH), 7.92 (d, *J*= 5.32 Hz, 1H PyH), 7.88 (m, 2H, PyH), 7.85 (s, 3H, ArH), 7.78 (d, *J*= 5.36 Hz, 1H, PyH), 7.50-7.65 (m, 3H PyH), 7.45 (t, *J*= 6.08 Hz, 2H, PyH), 1.42 (s, 54H, *t*-butyl); MALDI: calculated 1643.5593 ($C_{95}H_{96}Cl_2N_{12}RuZn$), observed 1543.6770 $[(Ru(7)(bpy)_2]^+Cl$.

1-[5-(1-phenyl)-10,15,20-tris(3,5-di-tert-butyl)phenylporphyrinyl]-1H-1,2,3-triazole-4-yl pyridine (7)

Porphyrin (7-Zn) (0.050 g, 0.043 mmoles) in CH_2Cl_2 (15 mL) was added HCl in dioxane (20 M, 2.5 mL), stirred at r.t. for 5 min. The mixture was neutralised with saturated $NaHCO_3$ solution, dried over sodium sulphate, and the solvent was removed under reduced pressure to yield the product in 90% yield (0.045g)

R_f : 0.4 ($CHCl_3$); UV Vis. ($CHCl_3$), λ_{abs}/nm (log ε): 424(5.57), 520(4.05), 557(3.75), 595(3.60), 651(3.66); ^1H NMR (400 MHz, Chloroform-*d*) δ ppm : 8.88-8.97 (m, 8H, βH), 8.71 (s, 1H, triazole H), 8.45 (d, *J*= 8.4 Hz, 2H, PyH), 8.39 (d, 2H, ArH), 8.24 (d, *J*= 8.4 Hz, 1H, PyH), 8.10 (m, 7H, ArH, PyH), 7.90 (t, *J*= 7.64 Hz, 1H, PyH,), 7.81 (s, 3H, ArH), 7.34 (t, 1H, PyH), 1.51 (s, 54H, *t*-butyl), -2.70 (br.s., 2H, -NH); ^{13}C NMR (100 MHz, Chloroform-*d*) δ ppm: 149.6, 148.8, 148.7, 143.5, 141.2, 137.3, 135.6, 131.9, 129.9, 129.8, 123.4, 121.7, 121.1, 120.7, 120.3, 118.7, 31.8, 35.1; ESI MS: calculated 1094.662 ($C_{75}H_{82}N_8$), observed 1095.6715 $(M+H)^+$, 548.3394 $(M+2H)^{2+}$.

1-[5-(1-phenyl)-10,15,20-tris(3,5-di-tert-butyl)phenylporphyrinyl]-1H-1,2,3-triazol-4-yl-pyridine-2,2'-bispyridine ruthenium(II) chloride (8)

Porphyrin (7) (0.040 g, 0.0365 mmoles) and cis-Ru(bpy)$_2$Cl$_2$ (6) (0.0523 g, 0.108 mmol) were added in a mixture of THF (6 mL) and EtOH (6 mL). The solution was then bubbled with N_2 for a few minutes, and heated to 85 °C. After refluxing 15 h, the solvent was removed under vacuum and the residue was chromatographed on neutral Al_2O_3 and the last brown band was collected, using $CHCl_3$:MeOH (v/v) = 10:1 as eluent (18 % yield ~ 10 mg).

R_f : 0.3 (10% MeOH : $CHCl_3$); UV Vis. ($CHCl_3$), λ_{abs}/nm (log ε): 295(4.71), 425(5.57), 521(4.05), 556(3.57), 596(3.60), 651(3.66); ^1H NMR (400 M Hz, Methanol-*d*) δ ppm : 8.83-8.65 (m, 10H, βH, PyH), 8.62-8.52 (m, 3H, PyH, triazolyl H), 8.48 (d, 1H, PyH), 8.37 (d, 2H, ArH), 8.25 (d, 1H, PyH), 8.2-8.1 (m, 6H, ArH,PyH), 8.05 (s, 6H, ArH), 7.96 (d, 1H, PyH), 7.93-7.84 (m, 3H, PyH), 7.78 (d, 1H, PyH), 7.64-7.5 (m, 5H, Py H), 7.48-7.42 (m, 2H, Py H) , 1.51 (s, 54

View Article Online
DOI: 10.1039/C6NJ01676F

H, *t*-butyl); MALDI: calculated 1578.6458 ($C_{95}H_{98}Cl_2N_{12}Ru$), observed 1480.7020 [$(Ru(7-N_2)(bpy)_2]^+$.

Acknowledgements

We are grateful to acknowledge the Council of Scientific and Industrial Research (CSIR), New Delhi, University Grants Commissions (UGC), New Delhi, for financial assistance and USIC, University of Delhi, and Prof. R. Nagarajan, Prof. Pawan Mathur for cyclic voltammetry measurements.

References

1. Komatsu, T.; Moritake, M.; Tsuchida, E. *Chem. Eur. J.*, 2003, **9**, 4626-4633.
2. a) Kalyanasundaram, K. Photochemistry of polypyridines and porphyrin complexes. London: Academic Press; 1992; b) Panda, M. K.; Ladomenou, K.; Coutsolelos, A.G. *Coord. Chem. Rev*., 2012, **256**, 2601–2627.
3. Imahori, H. *Bull. Chem. Soc. Jpn*. 2007, **80**, 621.
4. Sauvage, J. P.; Collin, J. P.; Chambron, J. C.; Guillerez, S.; Coudret, C.; *Chem. Rev*., 1994, **94**, 993-1019.
5. Togashi, T.; Izumi, A.; Kon, H.; Kanaizuka, K.; Ishizaki, M.; Miyake, R.; Chang, H. C.; Haga, M.; Sakamoto, M.; Kurihara M. *Chem. Lett*., 2014, **43**, 1201–1203.
6. LeGourriérec, D.; Andersson, M.; Davidsson, J.; Mukhtar, E.; Sun, L.; Hammarström, L. *J. Phys. Chem. A*, 1999, **103**, 557-559.
7. Liu, X.; Liu, J.; Pan, J.; Anderssonb, S.; Sun, L. *Tetrahedron*, 2007, **63**, 9195-9205 and references therein.
8. a) Schulze, B.; Schubert, U. S. *Chem. Soc. Rev.,* 2014, **43**, 2522; b) Struthers, H.; Mindt, T. L.; Schibli, R. *Dalton Trans*., 2010, **39**, 675–696; c) Crowley, J. D.; McMorran, D. A. *Top. Heterocycl. Chem*., **28**, 31-83; d) Elliott, P. I. P. in *Organomet. Chem.*, 2014, **39**, Ch 1, 1-25.
9. a) Fazio, M. A.; Lee, O. P.; Schuster, D. I. *Org Lett.*, 2008, **21**, 4979-4982; b) Miguel, G. D.; Wielopolski, M.; Schuster, D. I.; Fazio, M. A.; Lee, O. P.; Haley, C. K.; Ortiz, A. L.; Echegoyen, L.; Clark, T.; Guldi, D. M. *J. Am. Chem. Soc*., 2011, **133**, 13036-13054; c) Schuster, D. I.; Li, K.; Guldi, D. M.; Palkar, A.; Echegoyen, L.; Stanisky, C.; Cross, R. J.; Niemi, M.; Tkachenko, N. V.; Lemmetyinen, H. *J. Am. Chem. Soc*., 2007, **129**, 15973-15982; d) Natali, M.; Ravaglia, M.; Scandola, F.; Boixel, J.; Pellegrin, Y.; Blart, E.; Odobel, F., *J. Phys. Chem. C*, 2013, **117**, 19334−19345.
10. Wang, H. X.; Zhou, K. G.; Xie, Y. L.; Zeng, J.; Chai, N. N.; Li, J.; Zhang, H. L. *Chem. Commun*., 2011, **47**, 5747–5749.
11. a) Punidha, S.; Sinha, J.; Kumar, A.; Ravikanth, M. *J. Org. Chem*., 2008, **73**, 323-326; b) Shetti, V. S.; Ravikanth, M. *Eur. J. Org. Chem.*, 2010, 494–508.
12. Li, H.; Cheng, F.; Duft, A. M.; Adronov, A. *J. Am. Chem. Soc*., 2005, **127**, 14518.
13. Stengel, I.; Mishra, A.; Pootrakulchote, N.; Moon, S. J.; Zakeeruddin, S. M.; Grätzel, M.; Bäuerle, P. *J. Mater. Chem*., 2011, **21**, 3726.
14. Stengel, I.; Mishra, A.; Pootrakulchote, N.; Moon, S. J.; Zakeeruddin, S. M.; Grätzel, M.; Bäuerle, P. *J. Mater. Chem*., 2011, **21**, 3726-3734.
15. Kolb, H.C.; Sharpless, K. B. *Drug Discovery Today*, 2003, **8**, 1128-1137.
16. Lee, C. W.; Lu, H. P.; Lan, C. M.; Huang, Y. L.; Liang, Y. R.; Yen W. N.; Liu, Y. C.; Lin, Y. S.; Diau, E. W. G.; Yeh, C. Y. *Chem. Eur. J.*, 2009, **15**, 1403-1412.
17. Fletcher, J. T.; Bumgarner, B. J.; Engels, N. D.; Skoglund, D. A. *Organometallics*, 2008**, 27**, 5430-5433.
18. Chauhan, S.M.S.; Kumar, A.; Srinivas, K.A.; Mishra, M.K. *Indian Journal of Biochem and Biophys*, 2003, **40**, 429-438.
19. Lee, J.; Kim, Y.; Kang, S. K.; Choi, I.; Yi, J. *Korean J. Chem. Eng*., 2006, **23(3)**, 512-515.
20. Bryden F.; Boyle, R. W. *Synlett.*, 2013, **24**, 1978–1982.
21. a) Hohloch, S.; Schweinfurth, D.; Sommer, M. G.; Weisser, F.; Deibel, N.; Ehret, F.; Sarkar, B. *Dalton Trans.*, 2014, **43**, 4437-4450; b) Richardson, C.; Fitchett, C. M.; Keene, F. R.; Steel, P., *Dalton Trans*., 2008, 2534-2537.
22. Merckx, T.; Haynes, C. J. E.; Karagiannidis, L. E.; Clarke, H. J.; Holder, K.; Kelly, A.; Tizzard, G. J.; Coles, S. J.; Verwilst, P.; Gale, P. A.; Dehaen, W. *Org. Biomol. Chem*., 2015, **13**, 1654-1661.
23. Ryan, A.; Gehrold, A.; Perusitti, R.; Pintea, M.; Fazekas, M.; Locos, O. B.; Blaikie, F.; Senge, M. O. *Eur. J. Org. Chem*., 2011, 5817-5844.
24. Toma, H. E.; Araki, K. *Coord. Chem. Rev*., 2000, **196**, 307-329.
25. LeGourriérec, D.; Andersson, M.; Davidsson, J.; Mukhtar, E.; Sun, L.; Hammarström, L. *J. Phys. Chem. A*, 1999, **103**, 557-559.
26. Lo, W. K. C.; Huff, G. S.; Cubanski, J. R.; Kennedy, A. D. W.; McAdam, C. J.; McMorran, D. A.; Gordon, K. C.; Crowley, J. D. *Inorg. Chem*., 2015, 54, 1572-1587.
27. Liu, X.; Liu, J.; Jin, K.; Yang, X.; Peng, Q.; Sun, L. *Tetrahedron*, 2005, **61**, 5655–5662.
28. Bobby, H.; Escudero, D.; Hager, M. D.; Friebe, C.; Winter, A.; Gorls, H.; Altuntas, E.; Gonzalez, L.; Schubert, U. S. *J. Org. Chem*., 2010, **75**, 4025-4038.

View Article Online
DOI: 10.1039/C6NJ01676F

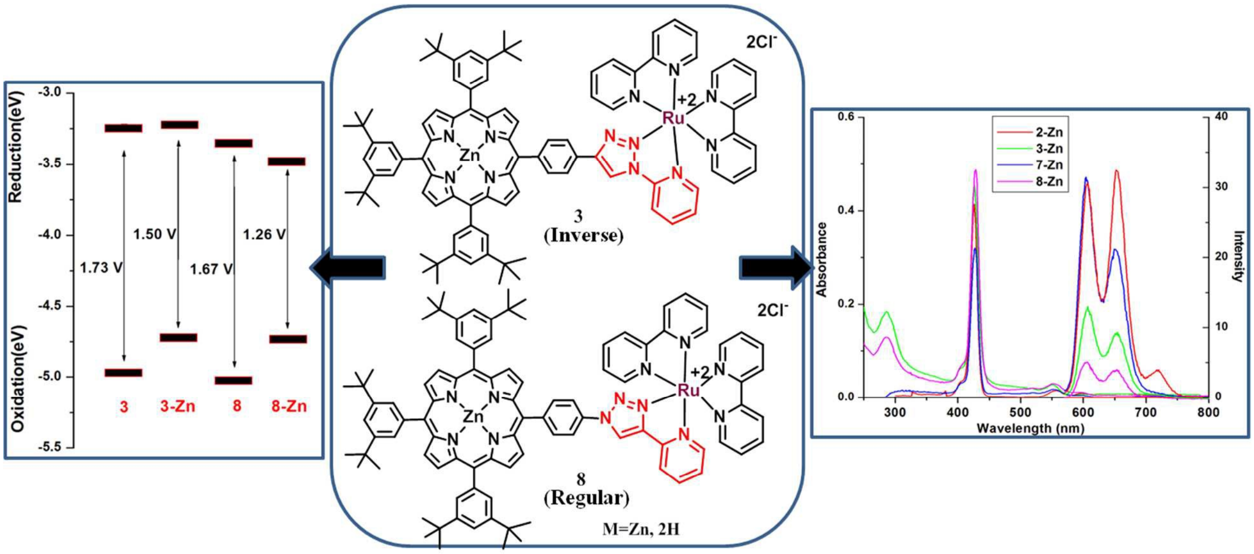

A family of inverse and regular triazolyl-pyridyl porphyrin-ruthenium(II) conjugates display an energy transfer from porphyrin to ruthenium bipyridyl moiety and a narrower HOMO/LUMO energy band gap which would help in increasing the electronic coupling, thus enhancing charge transfer in conjugates.